sciendo | Journal of Electrical Bioimpedance | JoEB bioimpedance.net

J Electr Bioimp, vol. 9, pp. 115-122, 2018
Received 9 Nov 2018 / published 28 Dec 2018
https://doi.org/10.2478/joeb-2018-0016

Extracting parasite effects of electrical bioimpedance measurements

Douglas Dutra [1], Pedro Bertemes-Filho [1,2]

1. *Department of Electrical Engineering, University of Santa Catarina State, Joinville, Brazil*
2. *E-mail any correspondence to: pedro.bertemes@udesc.br*

Abstract

The objective of this work is to develop a technique for filtering parasitic effects from the impedance spectra (IS) measured in biological material phantoms. IS data are contaminated with unexpected capacitive and inductive effects from cable, input/output amplifiers capacitances, electrode polarization, temperature and contact pressure when collecting data. It is proposed a model which contains an RLC-network in series with the Cole model (RSC), then called RLC-Cole. It was built four circuits composed by resistors, capacitors and inductors. An impedance analyzer (HF2IS) was used to perform the measurements in the frequency range of 1 to 3000 kHz. Data were fitted into the model and comparisons to the nominal values were made. In order to validate the proposed model, a gelatin phantom and a chicken breast muscle impedance spectra were also collected and analyzed. After filtering, Cole fitting was performed. Results showed a maximum root-mean-square error of 1% for the circuits, 2.63% for the gelatin phantom, whereas 2.01% for the chicken breast. The RLC-Cole model could significantly remove parasitic effects out of a tissue impedance spectrum measured by a 4-point electrode probe. This may be highly important in EIS systems whose objective is to discriminate a normal tissue from a cancerous one.

Keywords: Bioimpedance; Cole model; parasitic impedance; filtering algorithm

Introduction

Most electrical impedance spectroscopy (EIS) systems applies a constant amplitude alternate current to the sample by using two electrodes and the resulting voltage potential is measured between two other electrodes [1]. In order to assure a good characterization process, a current excitation system should cover a wide range of frequencies which may depend on the excitation technique and on the hardware characteristics [2]. An impedance is calculated and then a model of the studied sample is used for extracting the equivalent electrical parameters [3]. Digital processing may take place for filtering noise and performing calibration of the EIS system prior to impedance spectra calculation. Commercial EIS equipment may use two or four electrodes for impedance measurement, which may have or not have, cable effects compensation. Apart from this available compensation, commonly calibration can be applied externally by the user, such as short and open-circuit techniques. Due to the fact that four-electrode technique measures a transfer impedance, there has not been found in literature such a compensation technique in order to calibrate the measured data.

Impedance probes are the most common apparatus for performing EIS measurements [4–6]. Unexpected effects may occur during the measurements, such as electrode polarization, movement artefacts, uncontrolled applied force by the probe, temperature drift [7] sample contamination, cable impedance, parasitic capacitances [8], electronic constraints, and non-homogeneities, such as the one found in human tissues [9]. Controlling all those effects is a very difficult task, but important if a good extraction of the sample parameters are required [10]. In most cases, the high frequency impedance spectra are highly contaminated with cable and stray capacitance of the electronic [11].

The use of an electrical equivalent model in EIS, which best describes the material under study, is the ultimate goal of this technique. Modelling may give a wrong diagnosis, if the parameters do not represent the real biological properties of the material under study [12]. In general, the raw impedance data are fitted in a model. The fitting

process can be done using different techniques, such as Levenberg–Marquardt (LM) [13], particle swarm optimization (PSO) [14], genetic algorithm (GA) [15], and bacterial foraging optimization (BFO) [16]. However, the fitting process does not remove noise and parasitic effects from raw data, and hence an electrical model should represent the data including all those effects.
Characterization of biological tissue is difficult, as it cannot be modelled by a simple electrical equivalent circuit due to its anisotropy [17] and non-homogeneity. Phantoms have been used for mimicking biological materials in the field of electrical impedance spectroscopy [18], but also other properties of some materials, such as optical [19], mechanical and acoustic [20], anisotropy and visco-elasticity [21], thermal [22] and dielectric [23].

Most EIS system use the Cole model [24,25] for tissue characterization. This is a non-integer ($0 < \alpha < 1$) polynomial function (see equation 1) which best describes the biological sample. Different biological samples have a different α number. Most bioimpedance analysis consist of a resistance at zero frequency (R_0), a resistance at infinite frequency (R_∞), a dispersion coefficient (α) of the material under study and a relaxation time constant ($\tau = 1/2\pi f_C$).

$$Z(\omega) = R_\infty + \frac{R_0 - R_\infty}{1+(jf/f_C)^\alpha} \quad (1)$$

The higher is the frequency range (within a single dispersion) used in the measurements the better is the Cole fitting process, as it assumes resistance at both zero and infinity frequency. In practice, the electronic constrains the measurements into a narrow frequency bandwidth [26]. Furthermore, parasitic effects in the impedance data at higher frequencies limit the use of the Cole model as being an appropriate fitting technique.

A simple interpretation of the Cole equation can be represented in terms of a RSC electrical equivalent circuit (see figure 1c). It corresponds to the Fricke equivalent electrical circuit for the Cole equation, where R_2 represents the extracellular resistance in low frequencies ($R_2 = R_0$), $R_3 (= S)$ represents the intracellular resistance for high frequencies, and $R_\infty = R\,S\,/\,(R+S)$.

Parasitic effects introduce a "zero pole" in the Cole equation, resulting in an impedance increase with increasing frequency. Based on a literature review over the last 10 years, there are few published articles directly dealing with this modelling problem.

The objective of this paper is to investigate and propose an alternative equivalent electrical model for reducing the parasitic effects of measured bioimpedance data from the Cole equation. The validation of the model was investigated using phantoms of gelatin and chicken breast muscle.

Materials and methods

Impedance measurement setup

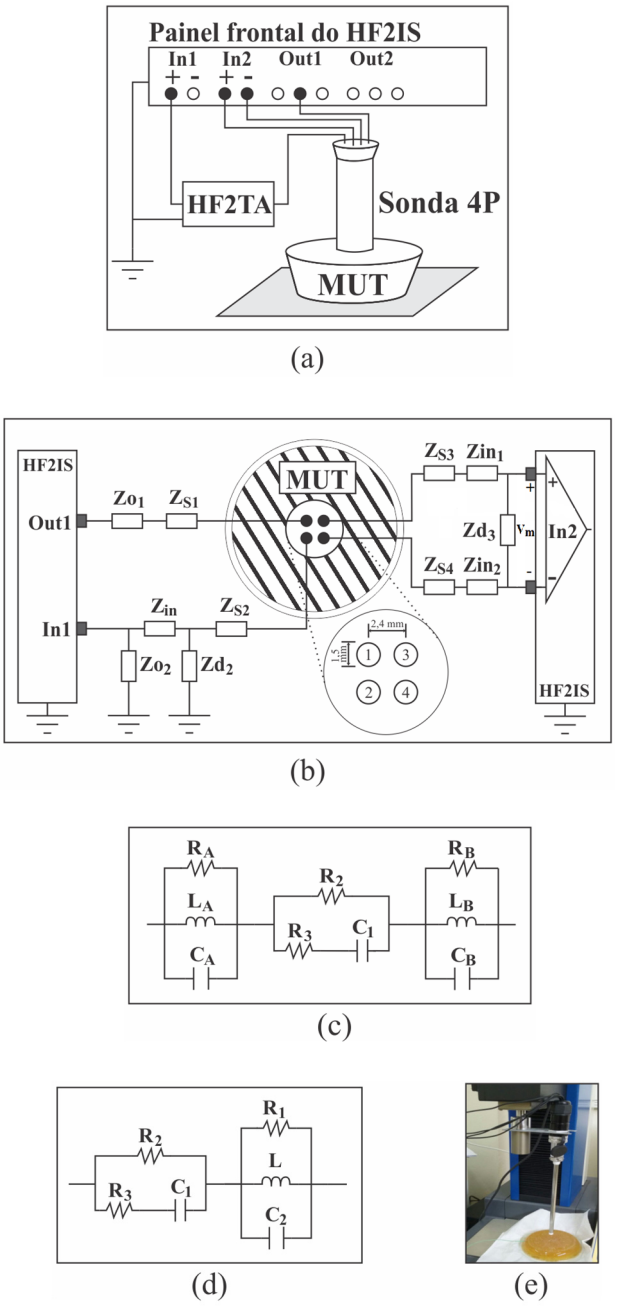

Fig.1: Schematic diagram of the model and measuring system. (a) Measuring system. (b) Parasitic impedances. (c) First proposed RLC-Cole-RLC model. (d) Final proposed RLC-Cole model. (e) Phantom measurements.

Measurements were performed by using an impedance meter (model HF2IS), a transimpedance amplifier (model HF2TA) and a homemade impedance probe. The output of the meter ($Out1$) in figure 1(a) was set up to provide a sinusoidal voltage of 2 Vpp (peak-to-peak) from 1 to 3000 kHz. The output voltage is converted to current by the HF2TA (transimpedance amplifier), which is recorded and averaged after 8 measuring frequency sweep.

Parasitic impedances

Even using the four electrode technique, residual electrode polarization effect may occur, especially if the electrode impedances are not completely balanced [12]. The proposed model may also compensate these effects. The objective of the proposed modelling technique is to extract only the properties of the material under study without the parasitic effects of the measuring system. Figure 1(b) shows the parasitic impedances Z_{S1}, Z_{S2}, Z_{S3} e Z_{S4} which are the contact impedances between the electrodes and the inputs of the measuring system (see the previous section). Zo_1 is the output impedance of the voltage to current converter, Zo_2 is the output impedance of the transimpedance amplifier HF2TA, Zd_2 and Zd_3 are the input differential impedance of the amplifier, $Zin_1$and Zin_2 are the input impedance of the amplifier.

Proposed equivalent model

The model shown in figure 1(c) is equivalent to the one of figure 1(d). Preliminary tests have shown similar results when extracting R_2, R_3 and C_1 from raw impedance data. The equivalent impedance shown in figure 1(d) can be calculated according to equations 2 and 3.

$$Z(\omega) = \frac{R_2\left(R_3+\frac{1}{j\omega C_1}\right)}{R_2+\left(R_3+\frac{1}{j\omega C_1}\right)} + \frac{\frac{j\omega R_1 L}{R_1+j\omega L}\cdot\frac{1}{j\omega C_2}}{\frac{j\omega R_1 L}{R_1+j\omega L}+\frac{1}{j\omega C_2}} \quad (2)$$

$$Z(\omega) = \frac{N(\omega)}{D(\omega)}. \quad (3)$$

$N(\omega)$ and $D(\omega)$ are polynomial functions that represent numerator and denominator respectively, and they are given by equations 4 and 5.

$$N(\omega) = -C_1C_2LR_1R_2R_3\omega^3 + j(LC_1(R_1R_2 + R_2R_3 + + R_1R_3) + LC_2R_1R_2)\omega^2 + (L(R_1 + R_2) + + C_1R_1R_2R_3)\omega - jR_1R_2 \quad (4)$$

$$D(\omega) = -C_1C_2LR_1(R_2 + R_3)\omega^3 + jL(C_1(R_2 + R_3) + C_2R_1)\omega^2 + (C_1(R_1R_3 + R_1R_2) + L)\omega - jR_1 \quad (5)$$

R_1, L and C_2 are parasitic values from the total measured impedance. Particularly, the inductor L represents the peak effect which may occur at high frequency.

Materials and Measurements

Four electrical circuits were built (see table 1) using resistors, capacitors and inductors. All components were previously measured. In order to connect the probe to the circuits, a circuit board was built. The penetration of the electrode in the sample was not tested, due to the fact that a surface electrode placed on the probe tip was used. The diameter of the impedance probe is 8 mm. The tip of the probe barely touched the material as far as an electrical contact was obtained.

The objective of using electrical circuits were to reproduce the increase of impedance magnitude at increasing frequency, and then to extract $R1$, L, $C2$, which were calculated from the fitted data. Standard deviations values are calculated in comparison to the measured ones. Furthermore, the Cole parameters ($R_0, R_\infty, f_C\ and\ \alpha$) are calculated, either for the measured or calculated ones (R_1, R_2, R_3, C_1, C_2 and L). A PSO algorithm was implemented in MATLAB for adjusting a known function to a set of experimental data, similarly as used in GA. However, PSO presents a faster convergence response to solve unrestricted problems with continuous variables [27], as for example the parameters from the RLC-Cole model.

Twenty measurements were made at three different points on a gelatin phantom, and then the RLC-Cole model parameters were calculated and averaged. The measuring points were placed 3 cm apart from one another. Two electrodes (1 and 2 in the figure 1(b)) are used for injecting current and two electrodes (3 and 4) for measuring the resultant voltage. The probe is both connected to the impedance meter and a universal force gauge (UFG) device (model DL-200 MF from EMIC), as it can be seen in the figure 1(e).

The UFG device was used in order to hold the probe in a vertical and steady state position, assuring a good contact between the probe electrodes at the gelatin surface. It also permits to push down the probe accurately until a soft force is applied to the gelatin and a voltage reading is visualized in the impedance meter. This assures a similar applied force for all measurements and then repeatability can easily be calculated.

The gelatin phantom was made of gelatin powder, agar-agar powder, sodium chloride (NaCl) and deionized water. It contains 25% of gelatin powder (50 g), 0.5% agar-agar powder (1 g), 74% of deionized water (148 ml) and 0.5% of NaCl (1 g), resulting in a total volume of 200 ml. It was kept in a glass bowl of 10 mm diameter. Measurements were collected at 25°C and repeated 20 times. Data were averaged and parameter values repeatability were calculated.

Table 1. Measured and fitted values for circuits 1 to 4, where NA means that the resonance frequency was not measured.

	Circuit 1		Circuit 2		Circuit 3		Circuit 4	
$\mathbf{C_1}$ **[nF]**	1.00	1.01	1.00	1.15	4.70	4.81	0.82	0.87
$\mathbf{R_2}$ **[Ω]**	56.8	55.8	50.5	50.4	73.3	80.5	65.2	67.5
$\mathbf{R_3}$ **[Ω]**	1.2	1.9	1.2	1.5	1.2	2.0	1.2	1.3
$\mathbf{R_1}$ **[Ω]**	1.1	1.5	1.1	0.7	242.0	294.0	61.9	61.0
L [μF]	100.0	101.0	2.7	2.5	80.0	109.0	15.0	17.3
$\mathbf{C_2}$ **[pF]**	0.0	0.001	15.0	18.0	271.0	221.0	271.0	350.0
$\mathbf{R_\infty}$ **[Ω]**	1.2	1.3	1.2	1.1	1.2	2.0	1.2	1.3
$\mathbf{f_C}$**[Hz]**	2.74	2.25	3.08	2.58	0.45	0.40	2.87	2.66
$\mathbf{f_R}$**[Hz]**	NA	9.60	25.00	22.80	0.34	1.03	2.50	2.02
RMSRE	**0.80**		**0.15**		**0.15**		**0.18**	

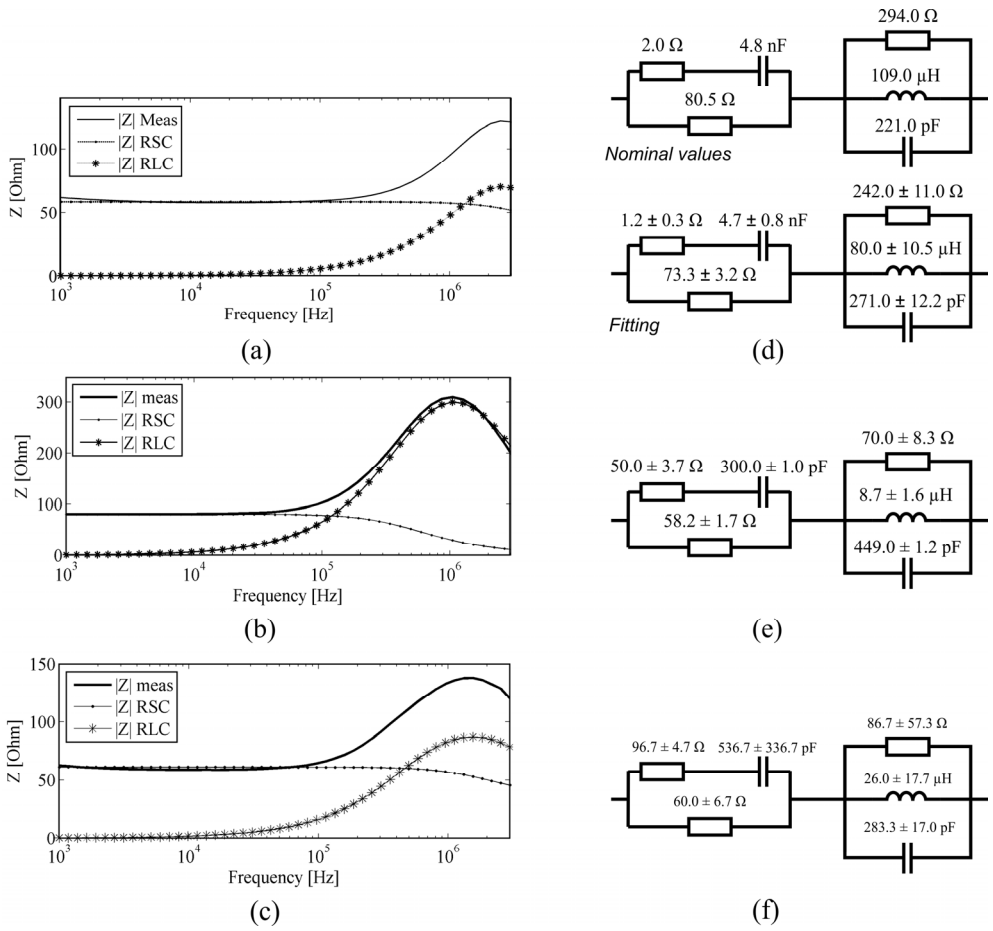

Fig.2: a) Mean impedance spectra of one of the electrical phantom; (b) gelatin phantom; (c) chicken breast muscle; (d) nominal and fitted values of the electrical phantom 3 (see table 1); e) fitted values for gelatin phantom; f) fitted values for chicken breast muscle.

Finally, measurements were made in a chicken breast muscle of approximately 150 × 95 × 25 mm and 200 g of weight. Applied force and temperature were controlled during the experiments. Measurements were collected at three different points on the chicken breast, and then repeated 20 times. The measuring points were also placed 3 cm apart from one another.

Ethical approval

The conducted research is not related to either human or animal use.

Results

Electrical phantoms

Table 1 shows both extracted and calculated parameters, where the first 6 ones were extracted. The root mean square of the relative error ($RMSRE$) was calculated according to equation 6 [28], in order to evaluate the effectiveness of the parasitic effects cancelation, simulated by the circuit RLC.

$$RMSRE = \sqrt{\frac{1}{n}\sum_{i=1}^{n}\left(\frac{Z_{MEAS_I} - Z_{RLC-Cole_i}}{Z_{RLC-Cole_i}}\right)^2} \qquad (6)$$

Figure 2(a) shows the spectra of one electrical circuit showing both Z_{RSC} and Z_{RLC} from the raw measured impedance. It can be seen that the effects start to appear from 100 kHz. The corresponding parameters are shown in figure 2(d).

The cutoff frequency was estimated to be 400 kHz whereas 450 kHz for the measured one.

Z_{MEAS} and $Z_{RLC-Cole}$ are the magnitude from measured and fitted impedance, respectively, for 50 points in the frequency range. The maximum error was 0.80% whereas 0.15% was the minimum, which might be related to the resonance frequency and, consequently, to the value of the inductor L in the RLC circuit. The higher the inductor L the higher the error appears to be. It was observed a value of approximately 0.86 for all four circuits tested here.

Gelatin and muscle data

The RLC-Cole parameters of the gelatin were collected 20 times at 3 different points over the frequency range of 1 to 3000 kHz. Each measured point of the gelatin contains 50 discrete frequencies. As a result, each impedance spectrum of each point contained 20 values for each discrete frequency which were averaged, and then the parameters of the proposed model were extracted. In addition, the mean parameters were also extracted for the mean impedance spectra. The RMSRE value at each measured point was

calculated. The mean values are shown in figure 2(e). The extracted cutoff frequency was 4.90 ± 0.19 MHz, resulting in a RMSRE of 2.05 ± 0.42%. The higher frequency values were measured in order to capture the parasitic effects within the sample.

Figure 2(b) shows the mean impedance spectra taken from 3 different points of the gelatine phantom, the total impedance and both Z_{RSC} and Z_{RLC}. It can be seen that the impedance Z_{RLC} does not affect the data until 100 kHz.

In order to test the proposed modelling in a muscle-type material, a chicken breast muscle was used. The RLC-Cole parameters at three different points of the chicken breast were collected and fitted. The same procedure for calculating the RMSRE in the circuit was also used for the muscle.

In contrast to gelatin phantom, the capacitance C_1 is different at different measured points, and, consequently, different f_C parameters. Each muscle site contains different structure and ion content, imposing different impedance spectra and combined parasitic effects on the measured data. The mean values found are shown in the figure 2(f), whereas R_∞= 37.0 ± 2.4 Ω, f_C = 2.74±1.43 MHz, f_R = 2.89 ± 1.84 MHz, α = 0.40 ± 0.02, and RMSRE = 1.81 ± 0.19%.

Discussion

The use of phantoms in electrical bioimpedance has been widely investigated due to its facility of mimicking an isotropic, homogeneous a semi-infinite medium [29]. The geometrical dimensions of the phantoms used in this work are similar to the ones used in others studies [30]. Phantoms are widely used to investigate the behavior of biological materials, such as optical, mechanical and electrical properties. The Cole model is mostly used to extract the electrical properties of the material by using different processing techniques, such as PSO, artificial network [31], and Non-Linear Least Squares [32]. This work used the PSO due to the fact that the convergence of the output is faster when it involves continuous variables like the Cole parameters [31].

The collection of impedance data from biological materials are usually done by homemade electrode probes, which are connected to EIS systems by using either coaxial or triaxial cables of approximately 50 cm length [33]. Such a connection introduces parasitic effects in the measured data [34,35] at high frequency. Nevertheless, other effects may happen at very high frequencies, such as the Hook effect, which looks like an inductive effect by increasing the measured impedance over that frequency range [33,35].

The results showed in figures 2(a), 2(b) and 2(c) have such parasitic effects at higher frequencies. It was expected that the impedance spectra should decrease at increasing frequency, especially above 500 kHz.

If we represent the impedance as a function of angular frequency (ω), then the increase in its magnitude at high frequency might be interpreted as a zero in the impedance polynomial function $Z(\omega)$ which, in turn, indicates an inductive effect over the impedance data. Impedance of biological material has been intensively studied over the last 50 years, and it has not been found such inductive behavior in this type of material. This might suggest that cables inductances, together with parasitic capacitances in series with the impedance of the material under study, pushing the modulus of the total impedance up at higher frequencies.

Many attempts have investigated the Hook effect over a transfer function at high frequency. One of this attempt modeled the human body using a cylindrical conductor of 10 cm with its screen grounded and modeling the behavior as a transmission line to extract the equivalent parameters [8]. The results of that study presented parasite capacitances of about 100 pF, which has the order of magnitude found in this work. Hook effects over the transfer function in a system might also be explained by coupling capacitances, feeding output to input. The feedthrough capacitances may impose "zeros" in the transfer polynomial of a such a measuring system. If so, those capacitances might be smaller than 10 pF and then having an insignificant effect over the impedance spectra, as far as the electrode impedance is smaller than 100 Ω. The measured electrode impedance in this work was in the order of 1 Ω. Nevertheless, the distance between electrodes placed on the probe surface was 2.4 cm, which may contribute to the appearance of some small feedthrough capacitances in the measuring system.

Therefore, parasitic effects were here modelled in terms of a parallel RLC circuit. The inductive effects act as a positive phase phenomenon in the impedance model, as described by Kalvøy *et al.* in 2015. They have showed that these specific effects are directly related to parasitic capacitance to ground which, in turns, do not depend on the type of electrode system (i.e., bipolar or tetrapolar). Therefore, the positive phase behavior in the measured data was numerically modelled here by an inductance L, as proposed by the RLC-network [37]. The total measured impedance was then modelled as a RLC circuit in series with an RSC one, where the latter represents the Cole model for the material under study. Most EIS system uses the Cole model for extracting the electrical properties of the material under study [38]. In order to improve the precision of the measuring device (HF2IS), calibrations were performed by using known resistors values and then Bode graphics were collected. Calibrated measured data were compared to a simulation performed in Matlab in order to proof precision of the system. The type of materials under test in this work do not present any relaxation process in the frequency range of interest, so the resonances due to the added network do not hide any information of the sample.

The first part of the experiments considered mimicking the parasitic effects over the impedance of the material under study. This was achieved by building equivalent circuits using known values of resistor, capacitors and inductors. Four different test circuits were built and an algorithm in MATLAB was developed for fitting purpose and extraction of components. The maximum root-mean-square relative error ($RMSRE$) was 0.8%, which can be considered low for such a type of modelling. Error will be decreased if more precise capacitors and inductors are used in the circuit. It was used capacitors of 20% tolerance, whereas 10% for inductors. Even thought, the calculated values of the components compared to the nominal ones were very similar to one another. This implies that the fitting process precisely filters the RLC effects from the total measured impedance. As a result, the cutoff frequency (f_C) of Z_{RSC} showed in figure 2(a) was calculated to be approximately 400 kHz, which is close to its original value of 450 kHz. The determination of the cutoff frequency in the Cole model is very important for the correct calculation of the equivalent capacitive effect of the material under study, which, consequently, may mislead the whole characterization. Therefore, without the filtering process proposed here, it was almost impossible to obtain the cutoff frequency of the material due to the presence of parasitic components mixed in the data.

Data shown in table 1 should be carefully analyzed. Although it shows good results, this might not be proof for real objects where the material is contacted by electrodes with long leads. First, the electrode contacts and the parasitic elements associated with it are quite variable and not real elements, such as gelatin phantoms and chicken breast tissue. Secondly, at least at higher frequency, cable behavior and reflection may comprise the interpretation of the measured results. Thirdly, the effect of the distance between the material and the ground of the measuring setup.

In the second part of the experiments, impedance spectra of gelatin were measured due to the fact that this type of material is highly isotropic and homogeneous. Furthermore, gelatin phantoms are important in biomedical research as they have been widely used for mimicking biological tissue behavior, and are easily fabricated with different conductivity and stiffness [39]. Gelatin phantoms are mostly composed of water but also contain salt to change their conductivity according to the application. Because of this, temperature drift is always a significant concern when measuring the impedance of this type of material. In order to assure a good data repeatability, temperature was measured before and after the measurements. The temperature variation along the experiments was smaller than 1°C. One type of gelatin was made, and measurements were collected 20 times at 3 different points. The extracted parameters were quite constant compared to the mean value.

Conductivity values of gelatin have been measured already and published over the last decade [23,39,40]. It was observed the presence of parasitic effects at higher frequencies (see figure 2(b)).

Based on a literature review over the last 10 years, there are little published data on the electrical properties R_0, R_∞, f_C and α from the impedance Cole equation of chicken breast muscle.

Nevertheless, data have already been published in the literature about the dielectric properties of fresh, unfreeze and cooked bovine and chicken meat [41,42]. The phantoms used in this work are considered as an isotropic, homogeneous and semi-infinite medium. On the other hand, biological tissues are anisotropic which may explain why the results of many published data are significantly different, such as the one found for bovine beef [42]. Anisotropy is related to the fiber distribution inside tissue, which impose more or less impedance for a certain direction of current flow [43].

The parameters extracted from chicken muscle have a significant influence of anisotropy, which was shown in terms of high standard deviation for C_1, R_1 and L. This explains why the standard deviation error was quite big for the α and f_C parameter, related to electrical phantoms. It is important to point out that the anisotropy is not a parasitic effect, but a material characteristic. We have not measured the chicken muscle impedance in multiple directions (i.e., longitudinal and transversal directions along the muscle fibers).

Care should be taken when using this model for measured beef data, as anisotropy was not considered and modelled here. It must also be emphasized that a four-electrode probe made of gold was used for collecting the data, therefore a two-electrode impedance spectrum may not be fitted into our model. It is also well known that tissue is composed of many layers with different mechanical and electrical properties. The impedance probe is put in contact with the tissue sample, and then a small applied pressure is necessary for a good contact. Different applied pressure will result in different impedance spectra. All data were performed at very light applied pressure. In the case of the gelatin phantom, a very small standard deviation error showed that the applied pressure did not play an important role.

It must be emphasized that this work did not incorporate effects such as mutual inductance between the injection and detection circuit in four-wire measurements and pseudo-inductances. Mutual inductance may arise from parasitic capacitances between the sample being measured and the environment, namely earth ground and grounded objects or even the human operator's body.

Results from tested circuits showed that the proposed technique is feasible and the gelatin experiment also showed a good repeatability with a small standard deviation error. Further investigations will be necessary for other types of impedance probe with different electrode geometry and measuring technique. A wider frequency range of data acquisition will be necessary in order to detect other tissue dispersions, which might need a more complex Cole model for taking into account two dispersions [23].

It can be concluded that the RLC-Cole model can significantly remove parasitic effects out of a tissue impedance spectrum measured by a 4-point electrode probe. This may be highly important in an EIS system whose objective is to discriminate a normal tissue from a cancerous one, which, in turn, may increase significantly both sensitivity and specificity of the measuring system.

Acknowledgements

To CAPES for the financial support of this work by means of a scholarship, registered under the number 00.889.834/0001-08, and UDESC for the institutional support.

Conflict of Interest

The authors declare that they have no conflict of interest.

References

1. Y. Zou and Z. Guo, "A review of electrical impedance techniques for breast cancer detection," Med. Eng. Phys., vol. 25, no. 2, pp. 79–90, Mar. 2003. https://doi.org/10.1016/S1350-4533(02)00194-7
2. S. Kun, B. Ristic, R. a Peura, and R. M. Dunn, "Real-time extraction of tissue impedance model parameters for electrical impedance spectrometer," Med. Biol. Eng. Comput., vol. 37, no. 4, pp. 428–432, Jul. 1999. https://doi.org/10.1007/BF02513325
3. A. S. Elwakil and B. Maundy, "Extracting the Cole-Cole impedance model parameters without direct impedance measurement," Electron. Lett., vol. 46, no. 20, p. 1367, 2010. https://doi.org/10.1049/el.2010.1924
4. R. P. Braun, J. Mangana, S. Goldinger, L. French, R. Dummer, and A. A. Marghoob, "Electrical Impedance Spectroscopy in Skin Cancer Diagnosis," Dermatol. Clin., vol. 35, no. 4, pp. 489–493, Oct. 2017. https://doi.org/10.1016/j.det.2017.06.009
5. R. J. Halter, A. Hartov, K. D. Paulsen, A. Schned, and J. Heaney, "Genetic and least squares algorithms for estimating spectral EIS parameters of prostatic tissues," Physiol. Meas., vol. 29, no. 6, pp. S111–S123, Jun. 2008. https://doi.org/10.1088/0967-3334/29/6/S10
6. J. Hilland, "Simple sensor system for measuring the dielectric properties of saline solutions," Meas. Sci. Technol., vol. 8, no. 8, pp. 901–910, Aug. 1997. https://doi.org/10.1088/0957-0233/8/8/011
7. E. T. McAdams, J. Jossinet, A. Lackermeier, and F. Risacher, "Factors affecting electrode-gel-skin interface impedance in electrical impedance tomography," Med. Biol. Eng. Comput., vol. 34, no. 6, pp. 397–408, Nov. 1996. https://doi.org/10.1007/BF02523842
8. H. Scharfetter, P. Hartinger, H. Hinghofer-Szalkay, and H. Hutten, "A model of artefacts produced by stray capacitance during whole body or segmental bioimpedance spectroscopy," Physiol. Meas., vol. 19, no. 2, p. 012, May 1998.
9. D. Miklavcic, N. Pavselj, and F. X. Hart, "Electric properties of tissues," Wiley Encycl. Biomed. Eng., vol. 209, pp. 1–12, 2006. https://doi.org/10.1002/9780471740360.ebs0403
10. D. Ayllón, R. Gil-Pita, and F. Seoane, "Detection and Classification of Measurement Errors in Bioimpedance Spectroscopy," PLoS One, vol. 11, no. 6, p. e0156522, Jun. 2016. https://doi.org/10.1371/journal.pone.0156522
11. K. Hollaus, O. Bíró, C. Gerstenberger, K. Preis, R. Stollberger, and B. Wagner, "Effect of stray capacitances on bio-impedances in quasi-static electric field," IEEE Transactions on Magnetics, 2005, vol. 41, no. 5, pp. 1940–1943. https://doi.org/10.1109/TMAG.2005.846218
12. S. Grimnes and Ø. G. Martinsen, Bioimpedance and Bioelectricity Basics, 2nd ed. Elsevier, 2008.
13. C. Grosse, "A program for the fitting of Debye, Cole–Cole, Cole–Davidson, and Havriliak–Negami dispersions to dielectric data," J. Colloid Interface Sci., vol. 419, pp. 102–106, Apr. 2014. https://doi.org/10.1016/j.jcis.2013.12.031
14. A. Paterno, L. H. Negri, and P. Bertemes-filho, "Efficient Computational Techniques in Bioimpedance Spectroscopy," Appl. Biol. Eng. - Princ. Pract., no. July, pp. 3–27, 2012.
15. R. Hassan, B. Cohanim, O. de Weck, and G. Venter, "A Comparison of Particle Swarm Optimization and the Genetic Algorithm," in 46th AIAA/ASME/ASCE/AHS/ASC Structures, Structural Dynamics and Materials Conference, 2005, pp. 1–13. https://doi.org/10.2514/6.2005-1897
16. S. Gholami-Boroujeny and M. Bolic, "Extraction of Cole parameters from the electrical bioimpedance spectrum using stochastic optimization algorithms," Med. Biol. Eng. Comput., vol. 54, no. 4, pp. 643–651, 2016. https://doi.org/10.1007/s11517-015-1355-y
17. T. Said and V. V. Varadan, "Variation of Cole-Cole model parameters with the complex permittivity of biological tissues," in 2009 IEEE MTT-S International Microwave Symposium Digest, 2009, pp. 1445–1448. https://doi.org/10.1109/MWSYM.2009.5165979
18. A. Pinto, P. Bertemes-Filho, and A. S. Paterno, "Gelatin as a skin phantom for bioimpedance spectroscopy," IFMBE Proc., vol. 49, no. 3, pp. 178–182, 2015. https://doi.org/10.1007/978-3-319-13117-7_47
19. P. Lai, X. Xu, and L. V. Wang, "Dependence of optical scattering from Intralipid in gelatin-gel based tissue-mimicking phantoms on mixing temperature and time," J. Biomed. Opt., vol. 19, no. 3, p. 035002, 2014. https://doi.org/10.1117/1.JBO.19.3.035002
20. M. Kavitha and M. R. Reddy, "Characterization of tissue mimicking phantoms for acoustic radiation force impulse imaging," IST 2012 - 2012 IEEE Int. Conf. Imaging Syst. Tech. Proc., pp. 553–557, 2012. https://doi.org/10.1109/IST.2012.6295585

21. M. D. Parker, M. Azhar, T. P. Babarenda Gamage, D. Alvares, A. J. Taberner, and P. M. F. Nielsen, "Surface deformation tracking of a silicone gel skin phantom in response to normal indentation," Proc. Annu. Int. Conf. IEEE Eng. Med. Biol. Soc. EMBS, pp. 527–530, 2012. https://doi.org/10.1109/EMBC.2012.6345984
22. M. P. Robinson, M. J. Richardson, J. L. Green, and A. W. Preece, "New materials for dielectric simulation of tissues," Phys. Med. Biol., vol. 36, no. 12, pp. 1565–1571, 1991. https://doi.org/10.1088/0031-9155/36/12/002
23. C. Marchal, M. Nadi, a J. Tosser, C. Roussey, and M. L. Gaulard, "Dielectric properties of gelatine phantoms used for simulations of biological tissues between 10 and 50 MHz," Int. J. Hyperth., vol. 5, no. 6, pp. 725–732, Jan. 1989. https://doi.org/10.3109/02656738909140497
24. K. S. Cole, "Permeability and impermeability of cell membranes for ions," Cold Spring Harb. Symp. Quant. Biol., vol. 8, no. 0, pp. 110–122, Jan. 1940. https://doi.org/10.1101/SQB.1940.008.01.013
25. D. D. Macdonald, "Reflections on the history of electrochemical impedance spectroscopy," Electrochim. Acta, vol. 51, no. 8–9, pp. 1376–1388, Jan. 2006. https://doi.org/10.1016/j.electacta.2005.02.107
26. J. G. Powles, "Cole-Cole plots as they should be," J. Mol. Liq., vol. 56, no. C, pp. 35–47, Jul. 1993. https://doi.org/10.1016/0167-7322(93)80017-P
27. L. H. Negri, P. Bertemes-Filho, and A. S. Paterno, "Computational Intelligence Algorithms for Bioimpedance-Based Classification of Biological Material," in IFMBE Proceedings, vol. 37, 2011, pp. 1229–1232. https://doi.org/10.1007/978-3-642-23508-5_318
28. B. A. Walther, J. L. Moore, and C. Rahbek, "The concepts of bias, precision and accuracy, and their use in testing the performance of species richness estimators, with a literature review of estimator performance," Ecography, vol. 28, no. 6, pp. 815–829, 2014. https://doi.org/10.1111/j.2005.0906-7590.04112.x
29. H. Kwon et al., "Bioimpedance spectroscopy tensor probe for anisotropic measurements," Electron. Lett., vol. 48, no. 20, 2012. https://doi.org/10.1049/el.2012.2661
30. C. Kim, A. Garcia-Uribe, S.-R. Kothapalli, and L. V. Wang, "Optical phantoms for ultrasound-modulated optical tomography," in Proceedings of SPIE, 2008, p. 68700M. https://doi.org/10.1117/12.766773
31. L. H. Negri, H. J. Kalinowski, and A. S. Paterno, "Benchmark for standard and computationally intelligent peak detection algorithms for fiber Bragg grating sensors," in SPIE Proceedings, 2011, vol. 7753, p. 77537F. https://doi.org/10.1117/12.885964
32. F. Seoane, R. Buendía, and R. Gil-Pita, "Cole parameter estimation from electrical bioconductance spectroscopy measurements," in 2010 Annual International Conference of the IEEE Engineering in Medicine and Biology Society, EMBC'10, 2010, pp. 3495–3498. https://doi.org/10.1109/IEMBS.2010.5627790
33. A. O. Ragheb, L. A. Geddes, J. D. Bourland, and W. A. Tacker, "Tetrapolar electrode system for measuring physiological events by impedance," Med. Biol. Eng. Comput., vol. 30, no. 1, pp. 115–117, 1992. https://doi.org/10.1007/BF02446203
34. T. J. Freeborn, T. Crenshaw, and S. Critcher, "Hook artifact correction of localized electrical bioimpedance for improved agreement between different device measurements," Biomed. Phys. Eng. Express, vol. 4, no. 1, p. 015016, Dec. 2017. https://doi.org/10.1088/2057-1976/aa971b
35. J. P. Reilly, "Applied Bioelectricity: From Electrical Stimulation to Electropathology," in Applied Bioelectricity, 1998, pp. 1–11.
36. R. Buendia, F. Seoane, and R. Gil-Pita, "A novel approach for removing the hook effect artefact from Electrical Bioimpedance spectroscopy measurements," in Journal of Physics: Conference Series, 2010, vol. 224, no. 1. https://doi.org/10.1088/1742-6596/224/1/012126
37. H. Kalvøy, C. Aliau-Bonet, R. Pallas-Areny, and Ø. G. Martinsen, "Effects of stray capacitance to ground in three electrode monopolar needle bioimpedance measurements," in Proceedings of the Annual International Conference of the IEEE Engineering in Medicine and Biology Society, EMBS, 2015. https://doi.org/10.1109/EMBC.2015.7320137
38. L. C. Ward, T. Essex, and B. H. Cornish, "Determination of Cole parameters in multiple frequency bioelectrical impedance analysis using only the measurement of impedances," Physiol. Meas., vol. 27, no. 9, pp. 839–850, Sep. 2006. https://doi.org/10.1088/0967-3334/27/9/007
39. M. A. Kandadai, J. L. Raymond, and G. J. Shaw, "Comparison of electrical conductivities of various brain phantom gels: Developing a 'brain gel model,'" Mater. Sci. Eng. C, vol. 32, no. 8, pp. 2664–2667, Dec. 2012. https://doi.org/10.1016/j.msec.2012.07.024
40. S. H. Oh et al., "Electrical conductivity images of biological tissue phantoms in MREIT," Physiol. Meas., vol. 26, no. 2, pp. S279–S288, 2005. https://doi.org/10.1088/0967-3334/26/2/026
41. M. Guermazi, O. Kanoun, and N. Derbel, "Investigation of long time beef and veal meat behavior by bioimpedance spectroscopy for meat monitoring," IEEE Sens. J., vol. 14, no. 10, pp. 3624–3630, 2014. https://doi.org/10.1109/JSEN.2014.2328858
42. J.-L. Damez, S. Clerjon, S. Abouelkaram, and J. Lepetit, "Dielectric behavior of beef meat in the 1–1500kHz range: Simulation with the Fricke/Cole–Cole model," Meat Sci., vol. 77, no. 4, pp. 512–519, Dec. 2007. https://doi.org/10.1016/j.meatsci.2007.04.028
43. J. A. Gómez-Sánchez, W. Aristizábal-Botero, P. J. Barragán-Arango, and C. J. Felice, "Introduction of a muscular bidirectional electrical anisotropy index to quantify the structural modifications during aging in raw meat," Meas. Sci. Technol., vol. 20, no. 7, p. 075702, Jul. 2009. https://doi.org/10.1088/0957-0233/20/7/075702